BABEȘ-BOLYAI UNIVERSITY, CLUJ-NAPOCA
FACULTY OF BIOLOGY AND GEOLOGY
DEPARTMENT OF GEOLOGY

DOCTORAL THESIS
Summary

Metallogenic Reinterpretations of the Epithermal Deposits Associated to the Neogene Volcanism in the Băiuț Metallogenic Field, Baia Mare District

PhD Supervisor
Assoc. Prof. PhD. *habil*. Călin Gabriel Tămaș

PhD student:
Réka Kovács

Cluj-Napoca
2024

Contents

Keywords: enargite, famatinite, luzonite, Breiner, Văratec, Cisma, Băiuț, Baia Mare metallogenic district

1. Introduction

The doctoral thesis entitled "*Metallogenic Reinterpretations of the Epithermal Deposits Associated with the Neogene Volcanism in the Băiuț Metallogenic Field, Baia Mare District* " was conducted under the scientific supervision of Assoc. Prof. PhD. *Habil*. Călin Gabriel Tămaș at the Doctoral School of Theoretical and Applied Geology, Babeș-Bolyai University in Cluj-Napoca. The present research aims to update the understanding of the eastern section of the Neogene Baia Mare Ore District, a significant concentration of polymetallic and subordinate gold – silver ores in Europe. The primary objective was to document, study, and identify the nature of the hydrothermal alterations and epithermal mineralization in the Băiuț ore field, specifically at the Breiner, Văratec, and Cisma ore deposits. Field research was conducted to identify and characterize the host rocks, the hydrothermal alterations, and the ores. Representative samples were collected for detailed mineralogical and petrographic studies, including multi-element chemical analyses and isotopic analyses of the lead within the ores. The results, gathered from 2017 to 2024, were presented at 6 scientific events and published in 7 specialized journals, 3 conference proceedings series and 4 abstract volumes. Three articles are published in Web of Science indexed journals.

2. Regional Geology

The Carpathians are part of the Carpathian-Pannonian region, linking the eastern Alps with the Balkans. This region consists of two microplates, Alcapa and Tisia (fig.2.1), separated by the "*Hungarian Median Line*" line/fault (Csontos and Nagymarosy, 1998). The Alcapa and Tisia microplates had distinct tectonic evolutions during the Mesozoic and Cenozoic, marked by opposite rotational movements and different translations (Csontos et al., 1992; Csontos, 1995; Seghedi et al., 1998; Márton et al., 1992; Pătraşcu et al., 1994; Panaiotu et al., 1996). The Carpathian arc resulted from the collision between the African and European plates during the closure of the Tethys Ocean (Royden, 1988; Csontos et al., 1992). The Neogene-Quaternary volcanic activity in the Carpatho-Pannonian region occurred on both Alcapa and Tisia microplates, forming a volcanic chain within Romania in the inner part of the Carpathian arc, forming the westernmost belt of the Eastern Carpathians.

The volcanic arc in the Eastern Carpathian is the result of subduction, collision, post-collision, and extension processes that occurred between the East European and Tisia-Dacia plates (Seghedi și Downes, 2011). The volcanic activity in the Carpathians began with felsic calc-alkaline volcanism in Eggenburgian (21-18 Ma, Aquitanian-Burdigalian), followed by intermediate felsic and calc-alkaline volcanism in Eggenburgian-Pannonian (18-8 Ma, Burdigalian-Tortonian), and concluded with Pliocene-Pleistocene alkaline basaltic volcanism in Pannonian-Cuaternar (10-0.1 Ma, Tortonian-Messinian). Seghedi and Downes (2011) classify the volcanic rocks from the Carpathian-Pannonian region into four groups based on SiO_2 vs. Na_2O+K_2O variations: calc-alkaline, Na-alkaline, K-alkaline, and ultra-K. The calc-alkaline group includes Miocene felsic pyroclastic rocks, Miocene to Quaternary calc-alkaline rocks, adakitic rocks with high Sr/Y ratios, and transition subgroups with high Nb content. Na-alkaline rocks formed monogenetic volcanic fields during the late Miocene to Quaternary. K-alkaline volcanism includes large-volume plateau volcanoes in the Styria Basin, while ultra-K volcanism is rare, represented by buried leucitite and lamproite volcanoes (Seghedi et al., 2008).

Two distinct types of volcanic activity have been identified in the Gutâi Mountains: 1) caldera-related acidic volcanism, which began around 15.4 million years ago (Fülöp, 2002, 2003), resulting in a complex array of ignimbrites and their redeposited equivalents in the southwestern portion of the volcanic area; and 2) intermediate multiphase volcanism, occurring between 13.4 and 7.0 million years ago (Kovacs and Fülöp, 2003), which led to the formation of various volcanic structures including composite volcanoes, extrusive domes, and intrusions (Kovacs et al., 2017). The complex metallogenetic activity of the Baia Mare district is associated to the intermediate volcanism, represented by basalts, rhyolites, andesites, basaltic andesites (Iancu & Kovacs, 2010). Key volcanic structures include andesite, dacite and basalts (Kovacs et al., 2017) associated with significant metallogenic activity. The Bogdan Vodă-Dragoș Vodă Fault, oriented east-west and located in the southern Gutâi Mountains, represents the easternmost section of the Hungarian Median Line (Csontos și Nagymarosy, 1998, Tischler et al., 2007) and has played a crucial role in forming mineral deposits in the Baia Mare metallogenic district, serving as a major structural control (Neubauer et al., 2005).

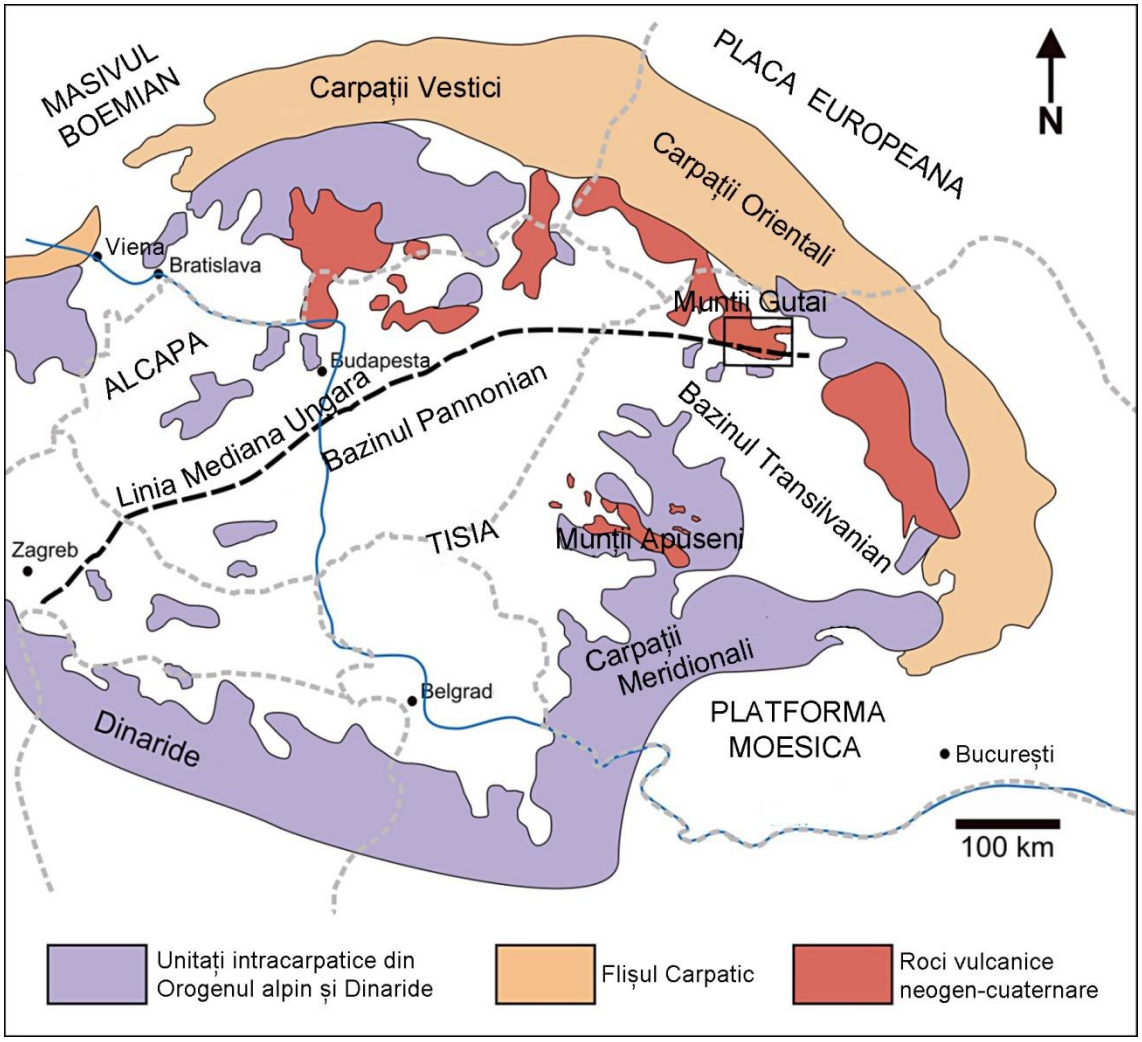

Fig. 2.1. Simplified geotectonic map of the Carpathian-Pannonian Region. The black rectangle indicates the location of the Gutâi Mountains (modified from Neubauer et al., 2005; Kovacs and Fülöp, 2010).

3. Geology of the Baia Mare metallogenetic district

The Baia Mare metallogenic district (fig.3.1) is situated in the southern part of the Gutâi Mountains and consists of tens of Pb-Zn-Cu and Au-Ag ore deposits (Borcoș et al., 1984). The location of the ore deposits within the district is structurally controlled by the east-west striking Bogdan Vodă-Dragoș Vodă fault system, located along the southern part of the Gutâi Mountains. Mining and drilling data, satellite images, and gravity anomalies indicate that the fault is partly obscured by Neogene volcanic rocks, though it is well exposed in the eastern section of the Baia Mare ore

district (Grancea et al., 2002). The magmatic control of the ore deposits is given by a pluton along the southern Gutâi Mountains, identified through geophysical and drilling results (Grancea et al., 2002).

The Baia Mare metallogenic district is divided into three sub-districts (Borcoș et al., 1974; Kovacs și Fülöp, 2010):

1. Ilba-Nistru (Pb-Zn-Cu±Au, Ag);
2. Săsar-Dealul Crucii (Au, Ag);
3. Herja-Băiuț (Pb-Zn-Cu and Au-Ag).

The ore deposits relate to the intermediate calc-alkaline volcanism and are considered by many authors to belong to the low-sulfidation, or transitional between low- and high-sulfidation. The ore bodies mainly occur as veins (Iancu și Kovacs, 2010; etc.), while stockworks, breccia dykes, and breccia pipes occur subordinately (Gurău et al., 1970; Tămaș, 2002; Iancu și Kovacs 2010), displaying clear geochemical vertical zoning (Manilici et al., 1965; Mârza, 2002; Mariaș, 2005).

Bailly et al. (1998) and Grancea et al. (2002) identified five stages of ore deposition in the Baia Mare district, as follows:

1. Fe stage with hematite, magnetite, wolframite, and scheelite;
2. Cu-Bi-(W) stage with chalcopyrite, pyrite, covellite, bismuth sulfides, and sulfosalts with rare gold;
3. Pb-Zn stage with sphalerite, galena, chalcopyrite, tetrahedrite, tennantite, and gold in quartz, adularia, illite/smectite, rhodonite, calcite, kutnohorite, and rhodochrosite gangue;
4. Sb stage with bournonite, tetrahedrite, stibnite, subordinate gold, and rare realgar and orpiment;
5. Au-Ag stage with gold, proustite/pyrargyrite, pearceite/polybasite, and native arsenic.

Radiogenic measurements indicate that the hydrothermal activity in the Baia Mare ore district is Pannonian in age (11.5-7.9 Ma; Lang et al. (1994) and Kovacs et al. (1997b). According to (Lang et al., 1994 and Kovacs et al. 1997b), the ore deposits in the Ilba-Nistru and Săsar-Dealul Crucii sub-districts are Lower Pannonian (11.5-10.0 Ma), while those in the Herja-Băiuț sub-district are Upper Pannonian (9.4-7.9 Ma). The age progression of the ore deposits from west to east mirrors

the volcanism age progression, with an approximate 1 Ma gap between volcanism and ore deposition (Mariaș, 2005).

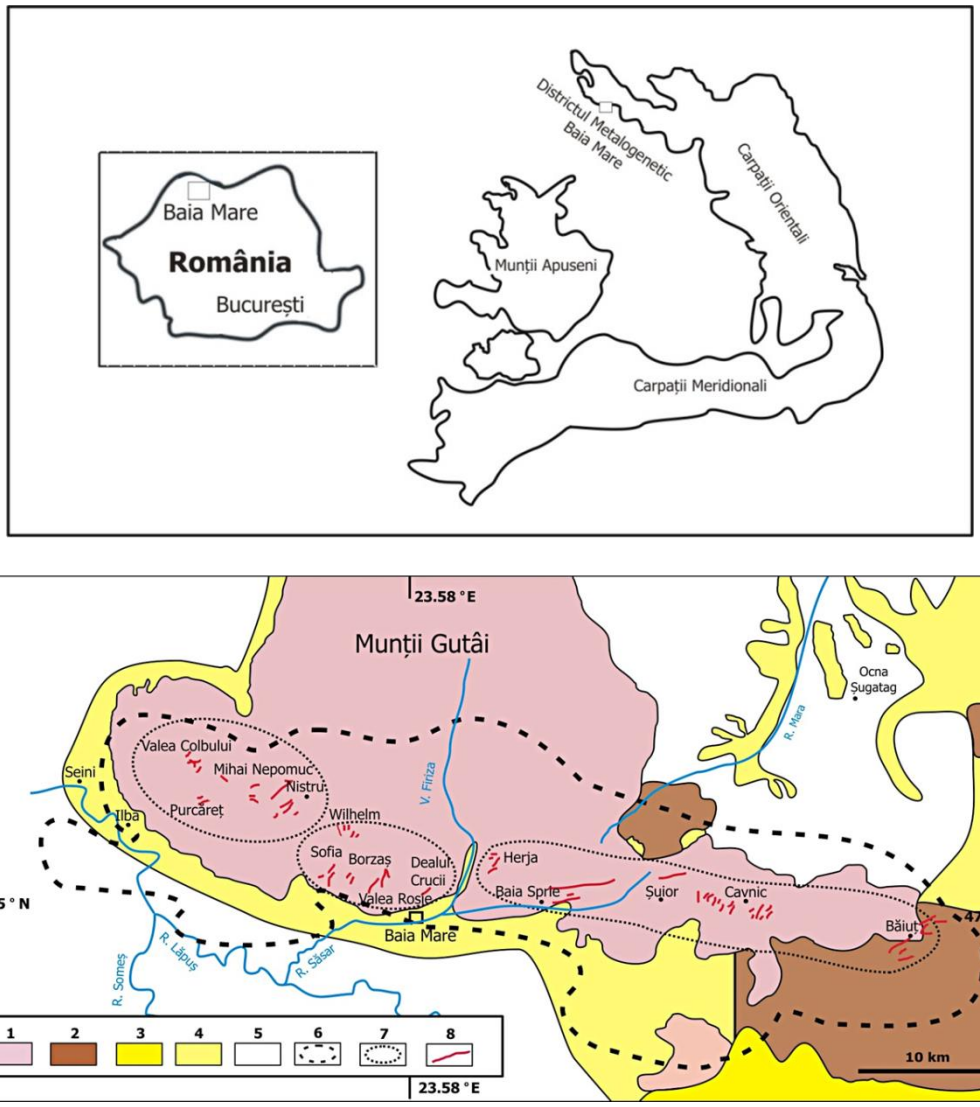

Fig. 3.1. The simplified geological map of the Baia Mare metallogenic district (redrawn after Kovacs and Fülöp in Iancu and Kovacs, 2010; Kovacs et al., 2017; Kovács and Tămaș, 2020) includes the following features: 1) Neogene volcanic rocks of the Gutâi Mountains; 2) Paleogene sedimentary rocks surrounding the Gutâi Mountains; 3) Oligocene-Miocene sedimentary rocks; 4) Neogene sedimentary rocks; 5) Quaternary sedimentary rocks; 6) Outline of the underlying pluton; 7) Metallogenic sub-districts (from west to east): Ilba-Nistru; Săsar-Dealul Crucii; Herja-Băiuț; 8) Ore bodies: veins, breccia bodies (dyke, pipe), stockwork.

4. Geology of the Băiuț ore field

The Băiuț ore field is located on the easternmost side of both the Herja-Băiut sub-district and the Baia Mare metallogenetic district (Iancu and Kovacs, 2010). The Băiuț ore field hosts three important ore deposits, i.e., Breiner-Băiuț (west); Văratec (central); Cisma/Poiana Botizei (east) (Borcoș and Gheorghiță, 1976).

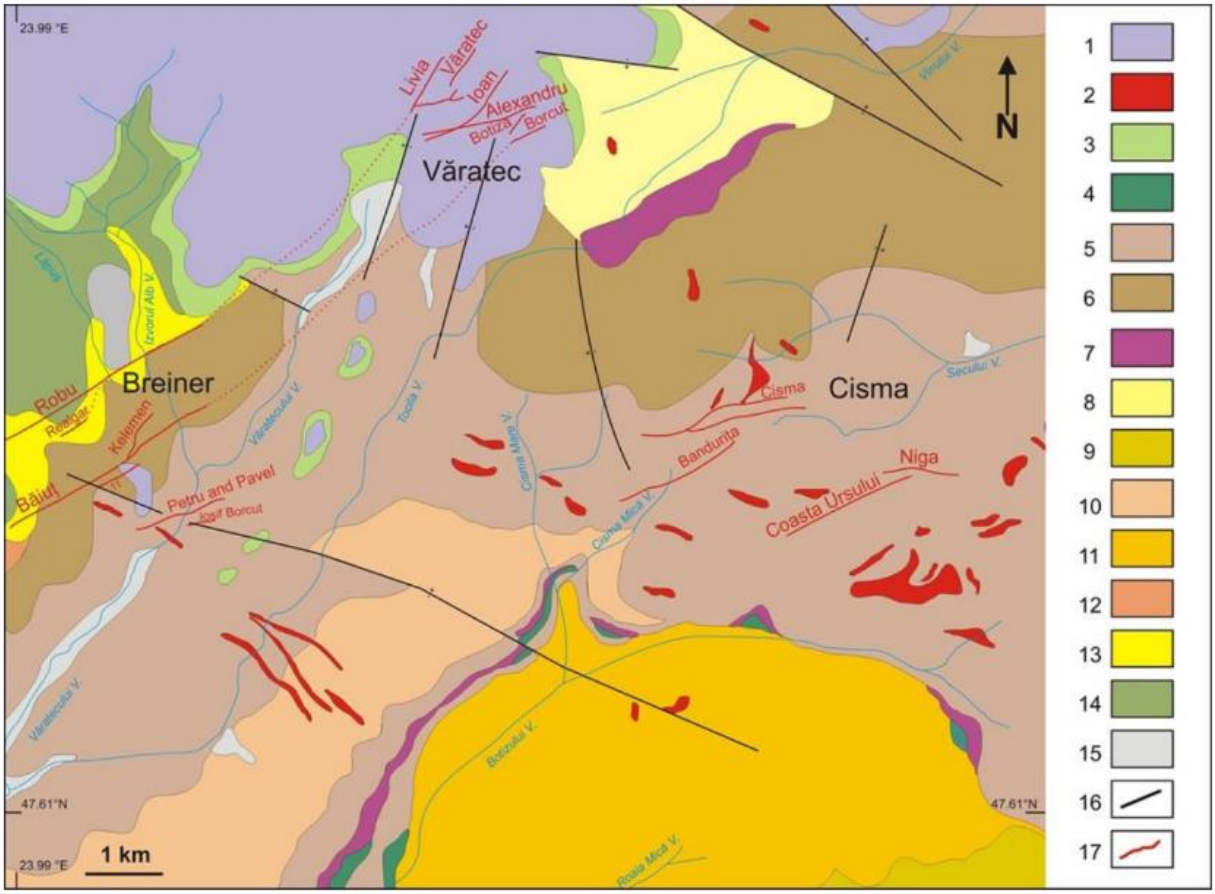

Fig. 4.1. Simplified geological map of the Băiuț metallogenic field (modified after Săndulescu and Russo-Săndulescu, 1981, and Mariaș, 2005; from Kovacs and Tămaș, 2020): 1) Pontian pyroxene andesites; 2) Neogene volcanic rocks; 3) Pontian (Odessian) volcano-sedimentary andesitic formations; 4) Senonian-Turonian brick-red marls and marly limestones; 5) Paleocene-Eocene sandy schist flysch; 6) Lutetian sandy flysch; 7) Paleocene-Eocene black and brown clays; 8) Priabonian sandy schist flysch; 9) Lutetian-Priabonian clays, marls, marly schists, sandstones; 10) Oligocene (?) sandstones and marls; 11) Lower Oligocene-Miocene sandy flysch with intercalations of marly sandy flysch; 12) Badenian sandstones and tuffs; 13)

Volhynian-Bessarabian marls and sands; 14) Odessian marls and sands; 15) Holocene deposits; 16) Faults; 17) Veins.

4.1. Geology of the Breiner ore deposit

The Breiner ore deposit is located at the western border of the Băiuț metallogenic field. According to Săndulescu and Russo-Săndulescu (1981) the Breiner ore deposit is defined by the presence of Paleocene-Eocene sandy schist flysch, Paleogene (Lutetian) sandy flysch, along with Neogene sandstones and tuffs (Badenian), Volhynian-Bessarabian and Odessian marls and sands, as well as Odessian marls and sands. The magmatic rocks are represented by microdiorites, andesites (Săndulescu and Russo-Săndulescu, 1981), while significant hydrothermal alterations such as silicification and sericitization have affected these rocks (Costin, 2000). The volcanic rocks were affected by a series of hydrothermal alterations represented by silicification, adularization, and sericitization (Costin, 2000). Key vein structures in the area, such as Petru și Pavel, Băiuț, and Robu, have been extensively explored, revealing several stages of mineralization (Mariaș, 2005; Edelstein et al., 1992). These stages include several deposition sequences, i.e., red-purple quartz with Fe oxides and pyrite, dark gray quartz with common sulfides, carbonates with galena and sphalerite, and quartz with barite and stibnite (Borcoș et al., 1977; Pop et al., 1982; Costin, 2000). The ore textures vary widely, with brecciated, banded, and massive forms among others, reflecting the diverse mineralizing processes that occurred at temperatures over 300°C (Manilici and Kalmár, 1973).

4.2. Geology of the Văratec ore deposit

The Văratec ore deposit, located in the central-western part of the Băiuț metallogenic field, consists of approximately 18 vein structures oriented NW-SE (Costin, 2007). Significant veins include TransLivia, Livia, Văratec, Radu-Vasile, and others, with the Livia vein considered an extension of the Robu vein from the Breiner-Băiuț area (Edelstein et al., 1992; Mariaș, 2005). The dip of these veins varies between 55° and 85° towards the NW, with an average of 70° (Costin and Vlad, 2005). The vein structures exhibit various textures such as banded, brecciated, massive, and cockade. Tectonic movements created fractures facilitating the emplacement of the subvolcanic bodies and the migration of the hydrothermal fluids (Costin and Vlad, 2005). The veins are hosted

by quartz microdiorites, andesites, Pannonian andesitic volcano-sedimentary formations, and Paleogene sedimentary rocks like Paleocene-Eocene sandy schist flysch (Mariaș, 2005; Borcoș et al., 1977; Săndulescu and Russo-Săndulescu, 1981). The veins contain native gold, common sulfides (predominantly pyrite, chalcopyrite, sphalerite, galena, and tetrahedrite-tennantite), and various sulfosalts including bournonite and members of the polybasite-pearceite series. Additional minerals, i.e. hematite, magnetite, siderite, calcite, malachite, cerussite, gypsum, barite, and anglezite have been mentioned by Costin (2007) and Costin and Vlad (2005). Borcoș et al. (1977) identified four stages of mineralization: 1) quartz, Fe oxides; 2) quartz, Fe oxides, pyrite, chalcopyrite, siderite; 3) quartz, Fe oxides, sulfides, adularia, siderite, kaolinite; 4) quartz, carbonates, marcasite. Significant hydrothermal alterations include adularization, silicification, carbonatization, as well as phyllic and propylitic alteration (Costin and Vlad, 2005). The Văratec ore deposit is characterized by a geochemical signature dominated by Pb, Zn, Cu, Au, Ag, Cd, Ni, V, Cr, Ti, Sb, As, Bi, and W (Costin, 2003). The hydrothermal fluids responsible for the ore deposition had temperatures ranging from 228.4°C to 356.6°C (Costin and Vlad, 2005).

4.3. Geology of the Cisma/Poiana Botizei ore deposit

The Cisma/Poiana Botizei deposit is the easternmost deposit in the Băiuț metallogenic field. This deposit consists of several vein structures, including Cisma, Bandurița, Prisăcele, Coasta Ursului, and Olimpiu (Borcoș and Gheorghiță, 1976; Damian et al., 2016; Istvan et al., 1995; Edelstein et al., 1992; Mariaș, 2005). The ore bodies are hosted by Paleocene-Eocene sandy schist flysch, which was intruded by Neogene quartz microdiorites and microgranodiorites (Săndulescu and Russo-Săndulescu, 1981; Plotinskaya et al., 2012). There are two distinct stages of mineralization identified in the Cisma deposit: 1) hematite, pyrite, chalcopyrite, tennantite, and tetrahedrite, ± sphalerite, galena, wolframite, and pyrrhotite; this stage also includes minerals from the lillianite-gustavite series and native bismuth (Damian and Damian, 2004); 2) galena, sphalerite, pyrite, chalcopyrite, marcasite, native gold, stibnite, realgar, orpiment, semseyite, boulangerite, and jamesonite (Damian and Damian, 2004). The vein textures are predominantly massive, with peripheral impregnations present in many cases.

5. Samples and analytical methods

The samples collected in the field are representative as they were collected from a large variety of rock and ore fragments within the waste dumps, and outcrops along the main valleys, slopes, and upper part of the massifs. On the waste dumps, the exposed material represents a mix of host rocks and ore samples mined out from the development and production mining works, and the selection of the samples allowed the collection of all available rock and ore types.

During the doctoral research, the following analytical methods have been used:

- optical microscopy in reflected polarized light;
- optical microscopy in transmitted polarized light;
- X-ray diffraction;
- geochemical analyses;
- scanning electron microscopy (SEM);
- electron probe micro-analysis (EPMA);
- lead isotope analyses.

6. Results in the Breiner ore deposit

In the Breiner deposit, various types of hydrothermal breccias were identified, characterized by different clast compositions and cement materials: 1) breccia with pyrite cement; 2) breccia with rounded clasts; 3) silicified breccia; 4) cockade breccia; 5) open-space breccia; 6) tectonically controlled breccia; 7) polymictic breccia; 8) breccias with massive pyrite clasts; 9) breccia with quartz-pyrite cement; 10) polymictic breccia with quartz cement.

Under the transmitted light polarizing microscope study revealed the presence of clay fragments, late carbonatation, which postdates the hydrothermal quartz cement. The host rocks are represented by fine-grained marls and coarser sandstones. These rock types occur as clasts within the hydrothermal breccias sometimes associated with metallic minerals, the most abundant being the pyrite. The hydrothermal breccias show sericitization.

In decreasing order of abundance, the mineral assemblage consists of pyrite, sphalerite, galena, chalcopyrite, and hematite, while the gangue minerals are represented by quartz and occasionally carbonates. The highest Au, Ag, and Cu grades occur in the hydrothermal breccias with pyrite

cement and in hydrothermal breccias with massive pyrite clasts. Significant contents of Au, Ag, Cu, Pb, and subordinate Zn are hosted by the quartz-cemented hydrothermal breccias and the breccias with pyrite (either as cement or clasts) containing quartz cement or cut by quartz veinlets (Table 6.1).

Table 6.1. Geochemical results on ore samples from the Breiner deposit.

Sample	**Au (ppm)**	**Ag (ppm)**	**As (ppm)**	**Cu* (ppm)**	**Fe (%)**	**Pb (ppm)**	**Sb (ppm)**	**Zn (ppm)**
5038	2.52	5.07	1180	1570	26.4	161	26.6	98
5039B	0.79	3.14	322	68.9	5.46	1320	28.8	152
5040B	1.92	25.1	1410	1.58 %	20.0	67.6	12.15	86
5040C	2.54	108	8280	7.27 %	22.9	4890	>10000	695
5041	1.64	4.81	351	439	4.95	308	92.3	896
5043	3.78	3.39	890	184	23.1	178.5	56.8	8
5044	6.15	43.4	1680	1.64 %	30.2	696	32	114
5047	0.29	0.79	162.5	119	3.73	159	23.3	507
5048	1.97	5.11	1040	789	19.15	209	18.2	19
5049	4.63	17.35	1155	814	13	860	37.6	2080

*For three samples, the content values are expressed in %, as per the notation, while for the remaining samples, the values are expressed in ppm.

7. Results of the Văratec ore deposit

7.1 Mineralisation of the Văratec ore deposit

Among the samples collected in the field, various types of materials specific to hydrothermal environment are included, namely: 1) banded ore with alternating sequences of pyrite and red quartz; 2) polymictic hydrothermal breccias with angular-subangular clasts of Paleogene sedimentary rocks and quartz cement; 3) tectonic/collapse breccias with quartz cement; 4) blocks of vuggy silica, specific to high-sulfidation systems; 5) open-space hydrothermal breccias with chalcopyrite and pyrite mineralization; 6) hydrothermal breccias with pyrite cement and angular clasts of Paleogene sedimentary rocks.

Optical microscopy observations revealed the occurrence of hydrothermal adularia present as characteristic idiomorphic rhombic crystals, intense sericitization, which postdates the hydrothermal quartz cement of the breccias, and carbonation. In decreasing order of abundance, the following metallic minerals were identified: sphalerite, chalcopyrite, hematite-magnetite, galena, pyrite, tetrahedrite-tennantite, and native gold. The ore microscopy study confirmed the presence of the native gold in the ores from the Văratec ore deposit. The native gold is predominantly associated with sphalerite or chalcopyrite. Another common mineralogical association of native gold is with hematite in quartz gangue. The size of the native gold grains ranges from 10 to 30 μm.

High concentrations of Au, As, Fe, and Sb (Table 7.1.1) are found in the massive banded ore with quartz gangue/cement containing hematite and pyrite. Samples with relatively high contents of Ag, Pb, and Sb were identified in hydrothermal breccia with quartz and pyrite cement; for example, the highest Cu and Sb grades were found in a hydrothermal breccia with quartz and pyrite cement.

Table 7.1.1. Geochemical results on ore samples from the Văratec ore deposit.

Sample	**Au (ppm)**	**Ag (ppm)**	**As (ppm)**	**Cu (ppm)**	**Fe (%)**	**Pb (ppm)**	**Sb (ppm)**	**Zn (ppm)**
5051	59.1	21.3	565	791	9.49	2760	32.6	7300
5054	1.85	158	246	1.47 %	11.85	3.44 %	18.2	1.02 %
5056	32	31	4330	9560	31.3	324	281	168
5058	0.24	122	821	4.72 %	12.3	7.24 %	824	1.01 %
5060	0.316	139	254	1.96 %	9.59	13.85 %	95	5.86 %
5064A	9.75	132	1405	2.53 %	25.3	2450	9.3	793
5064B	9.29	109	305	2.36	12.95	6.32 %	55.3	6450
5065	4.44	86.2	1340	7940	14.15	1.25 %	124.5	2.32 %
5070	0.88	196	75.2	3420	2.14	4.81 %	93.6	33
5075	23.2	48.6	59.8	1370	14.95	4300	25.4	92
5083	2.98	238	155	1560	9.79	19.1 %	145.5	142
5084	8.98	221	1210	2.9 %	19.6	12.6 %	85	162
5087	0.06	130	243	2.68 %	12.35	14.6 %	65	3.46 %

The EPMA results revealed that the analyzed native gold grains have gold grade ranging from 73.071 to 90.278 wt. % and the silver grade ranging from 10.145 to 24.448 wt. %.

7.2. Siliceous sinter

During the field research, several silicious sinter fragments were identified in the Văratec area, ranging from tens of centimeters to several meters in size. These were found along the Valea Albă, leading us to investigate the upper part of the massif to look for the source of these floats. After a difficult climb and passage through collapsed forest, a large erosion remnant landform was discovered. This erosional landform consists in a siliceous sinter deposit, measuring approximately 600 meters in length, 30-50 meters in width and several metes to maximum 18 m in height. The siliceous sinter deposit is located in the western sector of the Văratec mining perimeter.

The macroscopic examination in the field revealed several textural types of siliceous sinters i.e., 1) massive sinter deposits with supergene iron hydroxide imprints; 2) vuggy silica; 3) clast-supported breccias, interpreted as hydrothermal breccias; 4) massive sinters with rhythmic banding cut by hydrothermal breccias with white cement and clast-supported breccias; 5) centimeter to meter-sized banded siliceous sinter sequences.

The transmitted light optical microscopy allowed the identification of the nature of the sinter and several textural features, i.e., 1) silica sequences with extremely fine microcrystalline texture, cut by quartz veins; 2) globular textures formed of extra fine silica items; these globules are very finely crystallized on the outside border and progressively larger crystallized toward the inner part, ending with internal sequences of euhedral quartz crystals; 3) brecciated textures formed of fragments of microcrystalline silica embedded in hydrothermal quartz cement formed of well-defined quartz crystals, indicating the presence of brecciation that reworked the microcrystalline/cryptocrystalline silica material deposited during an earlier stage.

The geochemical results for the samples collected from the Văratec mining perimeter are summarized in Table 7.2.1 and indicate the following geochemical aspects:

1. sample 5148, a fragment of siliceous sinter with vuggy silica texture, has the highest contents of all analyzed metallic elements;
2. gold and silver grades are very low, except in sample 5148;
3. sample 5164, a highly dissolved siliceous sinter fragment, shows high concentrations of As (652 ppm), Sb (45.8 ppm), and Pb (43.9 ppm);

4. the copper-rich nature of the collected samples is confirmed by relatively high Cu content: 1170 ppm in sample 5148, while the other samples have very low values, ranging from 5.4 to 41 ppm.

Tabel 7.2.1. Geochemical results on siliceous sinter samples from the western part of the Văratec mining perimeter.

Sample	**Au**	**Ag**	**As**	**Cu**	**Fe (%)**	**Pb**	**Sb**	**Zn**
5148	61.9	22.5	1005	1170	13.1	1760	25.2	4950
5154	0.024	0.1	35.2	17.5	8.33	22.3	1.49	133
5155	0.011	0.06	29.6	6.9	0.94	41.1	10.1	9
5156	0.003	0.07	12.4	6.8	0.91	5.1	6.37	6
5157	0.007	0.04	26.2	4.6	1.16	9.5	11.4	14
5158	0.025	0.04	27.2	6.5	0.88	6	4.12	11
5159	0.061	0.04	54.8	8.8	1.18	8.8	7.64	8
5160	0.009	0.43	29.5	18.4	1.22	57.7	7.07	5
5161	0.003	0.03	9.2	5.4	0.68	5.6	1.99	4
5162	0.005	0.03	26.8	9.8	1.15	8.9	7.51	8
5163	0.01	0.03	29.2	41	1.18	10.9	7.57	10
5164	0.016	0.17	652	33.1	6.26	43.9	45.8	12

8. Results in the Cisma/Poiana Botizii ore deposit

The samples collected from the Cisma/Poiana Botizii ore deposit illustrate various types of mineralization and ores, i.e., 1) hydrothermal breccias with sedimentary rock clasts surrounded by rhythmic sulfides and quartz sequences; 2) brecciated polymetallic ore with quartz gangue; 3) hydrothermal breccias with pyrite cement and Paleogene sedimentary rock fragments, featuring open space breccias; 4) polymictic hydrothermal breccias with angular to sub-angular Paleogene sedimentary rock fragments; 5) vein structures with quartz gangue containing pyrite and chalcopyrite; 6) banded vuggy silica; 7) hydrothermal breccias with quartz amethyst cement; 8) breccias with rounded clasts held by a polymetallic hydrothermal cement with pyrite and hematite.

The most abundant and common metallic minerals macroscopically identified include pyrite, chalcopyrite, galena, and hematite; they are associated with hydrothermal quartz gangue.

The ore microscopy study of the ores from Cisma deposit led to the identification of a metallic mineral association consisting of chalcopyrite, hematite, galena, sphalerite, enargite, and tetrahedrite-tennantite as described by Kovács and Tămaș (2020).

The X-ray analyses carried out on selected metallic and gangue minerals from Cisma confirms the presence of kaolinite, and calcite, associated to galena.

The geochemical results obtained for the ore samples collected within the Cisma mining perimeter are presented in Table 8.1. These results acquired on 36 samples highlight several key findings, as detailed further:

1) gold is constantly present within the ores from Cisma, with only 9 samples showing concentrations below 0.1 ppm, while 13 samples exceeded 1 ppm, reaching a maximum of 4.78 ppm Au (sample 5168A). 2) high silver grades, especially in samples 5168A (487 ppm) and 5189 (226 ppm). 3) high copper content was identified in samples 5178 (2.09 %) and 5200 (2.63 %). 4) significant arsenic (As) content in sample 5175 (2020 ppm) and antimony (Sb) in sample 5168A (352 ppm); the highest lead grade of 5.48 % is carried by the sample 5168A.

The geochemical analyses results indicate higher concentrations of As compared to Sb, suggesting the possible presence of tennantite-type minerals from the tetrahedrite-tennantite group. High arsenic content across several samples, notably 5170 and 5178 (1920 and 2020 ppm As, respectively), indicate the potential presence of arsenic-rich minerals such as enargite (Cu_3AsS_4), previously confirmed in the Cisma deposit by Kovács and Tămaș (2018).

The sample 5178, which consists of massive ore with quartz and pyrite cement shows elevated levels of As (2020 ppm), Cu (2.09 %), and Fe (35.4 % Fe). Generally, the samples with relatively high contents of Ag, Pb, and Sb consist of ore fragments containing pyrite, chalcopyrite, and galena, e.g., sample 5168A with 487 ppm Ag; 5.48 % Pb; and 352 ppm Sb. The sample 5174 exhibits the highest Au grade, with 4.78 ppm, while the highest Cu grade is carried by a banded ore (sample 5200).

Table 8.1. Geochemical results on ore samples collected from the Cisma mining perimeter (Kovács and Tămaș, 2020). Content values are expressed in ppm except those indicated as "%".

Sample	Au	Ag	As	Bi	Cd	Cu	Fe	Mn	Pb	Sb	Se	Te	Zn
5167	0.12	0.43	134.5	2.2	3.06	96.8	9.45	4340	106.5	8.66	3	0.52	714
5168 A	1.37	487	1450	948	10.6	1.56 %	26.4	2020	5.48 %	352	110	13.1	363
5168 B	1.94	69.5	1190	106.5	791	7460	27	2000	2.31 %	17.6	21	1.96	16.5 %
5169	1.77	10.85	797	27	4.05	8220	23.5	269	163.5	11.5	50	3.5	756
5170	2.58	27.1	1920	85.1	4.75	1060	35.5	91	3530	23.5	26	3.45	910
5171	2.00	4.75	1410	20.8	4.81	407	28.3	390	409	4.84	18	1.82	929
5172	0.04	0.56	47.9	1.11	0.55	134	5.5	1120	84.8	3	2	0.52	194
5173	0.73	2.56	476	13.4	0.71	236	16.1	135	107.5	35.9	20	1.25	116
5174	4.78	7.78	944	38.1	0.28	1510	21.5	136	66.5	34	45	3.3	55
5175	2.56	4.25	595	21.8	0.38	752	15.75	319	62.9	29.2	28	2.08	80
5176	0.22	11.3	191.5	22.1	0.59	421	6.77	585	2000	11	6	0.65	117
5177	0.03	4.57	145	3.39	2.66	3940	5.62	3270	269	138.5	1	0.15	134
5178	2.33	32.6	2020	9.08	0.61	2.09 %	35.4	49	16.2	3.33	111	2.47	70
5179	1.29	15.25	1010	36.1	0.3	2360	32.2	78	106.5	6.93	50	1.76	59
5180	0.50	16.65	543	34.2	5.25	863	11.55	446	1900	8.66	9	0.94	1040
5181	0.05	5.39	215	7.28	13.45	2330	4.72	2320	727	262	2	0.28	608
5182	0.32	34.2	318	55.9	32.2	5080	7.86	173	5400	82.9	12	1.54	1260
5183	0.37	5.46	841	14.4	3.78	371	13.9	192	978	20.9	12	2.55	792
5184	0.02	1.5	136	1.06	1.8	1680	7.78	5920	127	118.5	1	0.1	104
5185	1.08	102	719	169.5	527	5130	19.8	965	4.13 %	16.5	<1	2.41	9.53 %
5186	0.33	12.7	917	19.75	11.75	5850	11.45	2700	1550	313	8	0.76	1120
5187	0.09	12.3	194.5	15.4	127.5	665	7.9	2310	9570	9.98	9	0.87	2.72 %
5188	0.78	31.5	843	7.58	207	1140	12.85	1300	5.06 %	29.6	16	0.68	3.67 %
5189	1.00	226	1110	451	14.1	1.66 %	29.7	1120	2.71 %	12.15	24	2.97	2000
5190	0.20	10.15	255	6.18	432	3390	8.63	1640	1660	5.79	5	0.35	9.65 %
5191	0.03	3.08	24.4	3.79	9.28	275	1.51	308	325	119	1	<0.05	2370
5192	1.82	21.7	888	19.05	1.2	6200	14.15	124	334	15.05	45	2.04	252
5193	1.87	11.85	1150	50.3	1.79	3010	22.3	97	505	12.6	24	1.58	370
5194	0.93	27.5	794	8.67	1.87	1.18 %	14.5	120	46.2	14.7	44	0.97	351
5195	0.03	1.99	22.1	2.85	1.13	324	1.25	129	147.5	25.8	2	0.15	259
5196	0.69	7.75	467	9.02	0.25	1440	11.55	118	32.9	11.8	23	0.96	55
5197	3.08	12.05	1050	47.9	0.44	6720	16	92	126.5	5.92	24	1.5	64
5198	0.07	20.2	89.4	45.6	0.44	840	1.95	134	1680	76.8	2	1.16	25
5199	0.85	3.01	321	12.25	0.12	856	8.61	118	83	5.98	11	0.89	24
5200	0.06	26.4	91.4	23.4	1.29	2.63%	8.37	861	100	12.5	8	1.1	108
5200 banded	0.06	13.6	93.6	169.5	0.61	8650	12.2	716	132.5	41.4	8	1.85	70

The scanning electron microscopy (SEM) study of the mineral assemblage including enargite/luzonite, tetrahedrite-tennantite, galena and chalcopyrite presented by Kovács and Tămaș (2020) using the semi-quantitative chemical data, confirmed the presence of the minerals identified earlier by ore microscopy.

SEM-BSE microphotographs revealed distinct shades of gray in enargite/luzonite grains, which correlate with variations of As and Sb content. Some grains show zoning with an outer whitish rim (Kovács and Tămaș, 2020). Minor variation in shades of enargite/luzonite indicates small chemical variations within a given mineral grain.

The EPMA provided quantitative chemical data for enargite/luzonite grains and a series of sulfides. The analyzed sphalerite grains contain apart Zn and S minor quantities of other chemical elements such as Fe, Cd, Cu, and Mn, collectively not exceeding 4.2 wt%. The average calculated chemical formula for sphalerite is $(Zn_{0.91},Cu_{0.004},Fe_{0.05},Cd_{0.01},Mn_{0.001},As_{0.0003})\Sigma=_{0.97}S_{1.03}$.

The EPMA results for chalcopyrite revealed nearly ideal values for Cu, Fe, and S. The calculated chemical formula of the analyzed chalcopyrite is $Cu_{0.99}Fe_{1.00}S_{2.01}$. The EPMA data obtained for the mineral grains of the tetrahedrite-tennantite series indicates higher average values for As (17.38 wt%) compared to Sb (2.17 wt%), with heterogeneous chemical compositions ranging between 15.48 – 18.10 wt% for As, and 1.67 – 3.12 wt% for Sb.

Tennantite systematically contains Ag, with the silver content ranging between 0.35 and 0.60 wt%. The calculated average chemical formula of the analyzed tennantite is $(Cu_{10.22},Fe_{1.76},Ag_{0.07},Pb_{0.05},Cd_{0.01})_{\Sigma=12.11}\ (Sb_{0.26},As_{3.43})_{\Sigma=3.69}\ S_{13.20}$.

Using the electron microprobe analyses, a number of 15 valid spot chemical analyses were obtained for enargite/luzonite, illustrating chemical variations. The analyzed enargite shows variable As content ranging from 12.07 to 17.96 wt%, as well as variable Sb content ranging from 0.27 to 8.74 wt%. The calculated chemical formula for enargite is $(Cu_{2.97},\ Fe_{0.06},\ Zn_{0.004})_{\Sigma=3.03}(As_{0.80,}\ Sb_{0.14})_{\Sigma=0.94}\ S_{4.03}$ (Kovács and Tămaș, 2018).

9. Lead isotopic compositions

Lead isotopic ratios ($^{206}Pb/^{204}Pb$, $^{207}Pb/^{204}Pb$, $^{208}Pb/^{204}Pb$) were obtained for the ores within the Băiuț metallogenic field and are presented in Table 9.1.

Regarding the Văratec ore deposit, the isotopic ratios of the two analyzed ore samples are distinctly different. One of these (sample 5051), exhibits the most radiogenic isotopic composition in the

entire Băiuț mining field ($^{206}Pb/^{204}Pb$: 18.88; $^{207}Pb/^{204}Pb$: 15.7; $^{208}Pb/^{204}Pb$: 39.2), while the second sample (5060) shows lead isotopic ratios falling between those obtained for the Breiner ores ($^{206}Pb/^{204}Pb$: 18.69-18.72; $^{207}Pb/^{204}Pb$: 15.61-15.65; $^{208}Pb/^{204}Pb$: 38.6-38.79) and those from Cisma ($^{206}Pb/^{204}Pb$: 18.23-18.32; $^{207}Pb/^{204}Pb$: 15.26-15.29; $^{208}Pb/^{204}Pb$: 37.92-37.93), specifically 18.52 for $^{206}Pb/^{204}Pb$, 15.46 for $^{207}Pb/^{204}Pb$, and 38.26 for $^{208}Pb/^{204}Pb$.

The ores from the Cisma deposit exhibit the least radiogenic isotopic ratios within the Băiuț metallogenic field ($_{206}Pb/_{204}Pb$: 18.23; $_{207}Pb/_{204}Pb$: 15.26; $_{208}Pb/_{204}Pb$: 37.93).

Table 9.1. The lead isotopic ratios ($^{206}Pb/^{204}Pb$, $^{207}Pb/^{204}Pb$, $^{208}Pb/^{204}Pb$) of the polymetallic sulfide ores from the Băiuț mining area.

Sample	Ore deposit	$^{206}Pb/^{204}Pb$	$^{207}Pb/^{204}Pb$	$^{208}Pb/^{204}Pb$
5041	Breiner	18.69	15.65	38.6
5049		18.72	15.61	38.79
5051	Văratec	18.88	15.7	39.2
5060		18.52	15.46	38.26
5168B	Cisma	18.23	15.26	37.93
5185		18.32	15.29	37.92

10. Interpretations

Breiner

The current study provides a detailed description of various types of ores collected during the field work within the Breiner ore deposit. It highlights the presence of a wide variety of mineralized breccias with diverse relationships between cement, clasts, and open spaces. The existing literature lacks mentions of breccias and related information, such as descriptive and genetic types of breccias, brecciation mechanisms and associated mineralization and ore mineralogy and hydrothermal alterations within the Breiner ore deposit.

The presence of brecciated, banded, and massive vein structures with vuggy silica textures, both in vein and in the wallrock, has been previously noted in the Breiner area by Borcoș and Gheorghiță (1976), as well as by Costin (2000).

In terms of hydrothermal alterations identified by the microscopy observation, we note the presence of silicification associated to the hydrothermal quartz cement. Considering the direct genetic relationship between hydrothermal brecciation and quartz cement, the silicification is considered a syn-brecciation hydrothermal alteration. The transmitted light microscopy allowed us to identify the carbonation. This hydrothermal alteration is late, occurring after the deposition of the hydrothermal quartz cement, as carbonates cover euhedral to subhedral hydrothermal quartz crystals within the breccia cement. The presence of minerals identified by ore microscopy in samples collected from the waste dump associated with the Breiner deposit confirms the observations made by Borcoș and Gheorghiță (1976), as well as Costin (2000).

Considering the succession of the ore mineral deposition at the scale of the metallogenic district and the mineralogy results obtained for the Breiner perimeter, the analyzed hydrothermal breccias formed primarily during the stage 1 (hematite+pyrite) and, less frequently during the stage 2 or 3 (common sulfides) defined by Bailly et al. (1998) at the Baia Mare District scale.

The geochemical analyses carried out on the samples from the Breiner area revealed that the highest precious metals and common metals grades are carried by:

i) the hydrothermal breccias with quartz veins cutting semi-massive pyrite mineralization (sample 5040 C), which show the highest contents of Ag, Cu, As, Sb, and Pb (108 ppm, 7.27%, 828 ppm, >10000 ppm, and 4890 ppm);

ii) the hydrothermal breccias with massive pyrite fragments and quartz cement have the highest contents of Au and Fe (6.15 ppm and 30.2%, sample 5044);

iii) highly silicified polymictic hydrothermal breccias (sample 5049) have relatively high Au grade (4.63 ppm) and the highest Zn content (2080 ppm).

The Ag signature of the Breiner ore deposit is confirmed by its constant presence within the analyzed samples. Although Ag values are nominally higher than those of the gold, economically, they are modest. Only one out of ten analyzed samples, exceeds 100 ppm Ag, specifically 108 ppm, while the remaining range between 0.79 and 43.4 ppm Ag. The previously known maximum Ag content for Breiner ore was 42.23 ppm (Costin, 2000). The polymetallic nature of` the Breiner deposit is evident from the high concentration of common metals, with maximum values of 7.27 % Cu, 4890 ppm Pb, and 2080 ppm Zn, significantly surpassing previous records of 1.04% Cu, 1.44% Pb, and 1.33% Zn (Costin, 2000).

The sample with the highest Cu content also contains the highest grade of As (8280 ppm) and Sb (>10000 ppm), suggesting the presence of copper-bearing minerals like tetrahedrite-tennantite and/or enargite/luzonite. Generally, the As content of the analyzed samples is one to two orders of magnitude higher than the Sb content, except the sample 5040C. The predominance of As over Sb indicates a tendency towards tennantite in the tetrahedrite-tennantite series and towards enargite/luzonite in the enargite/luzonite-famatinite series. The high Sb content in sample 5040C may also indicate the presence of stibnite.

Văratec

The present study presents the mineralized breccias from a descriptive and genetic perspective, thus highlighting the omnipresence of hydrothermal breccia structures in this deposit.

The sequence of hydrothermal alteration formation in the ores from Văratec is silicification, adularization, sericitization, and carbonatization.

Costin (2003) states that the Văratec deposit belongs to the third stage of mineralization deposition among the four stages defined by Borcoș et al. (1977), as follows: (1) quartz, Fe oxides; (2) quartz, Fe oxides, pyrite, chalcopyrite, siderite; (3) quartz, Fe oxides, sulfides, adularia, siderite, kaolinite; (4) quartz, carbonates, marcasite. The present study confirms the observations made by Borcoș et al. (1977) and Costin (2003) by identifying pyrite, chalcopyrite, sphalerite, galena, tetrahedrite, quartz, adularia, hematite hosted by quartz gangue, magnetite. Additionally, native gold was identified within the ores from the Văratec deposit. Considering the mineralogy revealed by optical microscopic study, the ores from the Văratec deposit match to the third stage of mineralization defined by Borcoș et al. (1977), with sulfides, adularia, and native gold, and correspond to stages 1 and 3 defined by Bailly et al. (1998).

The geochemical analyses of the ore samples collected from the Văratec deposit revealed several chemical peculiarities of the ores, as follows:

i) banded ore, with alternating sequences of pyrite and red quartz (sample 5051), possesses the highest gold content, reaching 59.1 ppm;

ii) massive polymetallic ore, dominated by the presence of pyrite and galena (sample 5083), shows the highest grades of silver and lead, at 238 ppm and 19.1 %, respectively;

iii) the ore with chalcopyrite and tetrahedrite-tennantite (sample 5056) has the highest content of arsenic and iron, at 4330 ppm and 31.3 %, respectively;

iv) the ore with galena, sphalerite, and chalcopyrite (sample 5058) presents the highest antimony and copper content, at 824 ppm and 4.72 %, respectively.

The geochemical analyses of the samples collected from the Văratec perimeter revealed the highest gold grade of 59.1 ppm (sample 5051). Additionally, the grade of 6 ore samples out of 13 exceeds 8 ppm. These results suggest the auriferous nature of the Văratec deposit and that the presence of native gold appears to be a common mineralogical and geochemical feature within the hydrothermal breccias.

The argentiferous signature of the Văratec deposit is indicated by the frequent presence of silver in the analyzed samples. For example, from 13 analyzed samples, 9 of them exceed a content of 100 ppm Ag, with the maximum value being 238 ppm, while the remaining range between 21.2 and 86.2 ppm Ag.

The results of the EPMA analyses of the native gold grains show that the chemical composition of the native gold grains is relatively homogeneous at the grain scale. However, there are significant compositional variations between the grains, which point out that there are three compositional types of native gold based on their silver content, as follows:

i) the first compositional type of native gold is characterized by the highest silver (24,99 wt.%) content, the silver content of this compositional type of native gold exceeds the maximum values reported by Costin and Vlad 2005;

ii) the second compositional type of native gold has an Au-Ag composition within the range mentioned by Costin and Vlad (2005): 16,75-18,49 wt.% Ag and 12,27-15,25 wt.% Ag.

iii) the third compositional type of native gold has the highest gold (90,268 wt.%) and lowest silver content (10,280 wt.%).

Overall, the mineralogy and geochemical results obtained for the ores from the Văratec perimeter allow us to consider it an auriferous and polymetallic ore deposit, with silver by product.

Siliceous Sinter

Compared to the sinter deposits described by Mariaș (2005) in the Cavnic area, the Văratec Vest sinter is significantly larger, measuring 600 meters in length and 30-50 meters in width. The macroscopic appearance of the Văratec sinter shows a variety of textures such as massive, banded,

vuggy silica, clast-supported, and open-space breccias, confirming the observations of White and Hedenquist (1995) and Mariaș (2005).

Transmission optical microscope observations indicate extra fine deposits of silica and globular textures, supporting the presence of nano- and micro-sized silicon spheroids, as argued by Rodgers et al. (2004) and Lynne et al. (2007). The silica undergoes morphological and structural changes depending on thermodynamic conditions, fluid recirculation, and other factors.

Geochemical analyses of samples from Văratec Vest sinter show significant contents of As (9.2-1005 ppm), Sb (1.49-45.8 ppm), and Cu (4.6-1170 ppm), with sample 5164 having the highest values. Generally, the Au and Ag contents are minor, except for the sample 5148 collected from a large allochthonous sinter block identified in Valea Albă, which has 61.9 ppm Au and 22.5 ppm Ag..

Compared to the Piatra Malnaș sinter (Mariaș, 2005), the Văratec Vest sinter has lower Au but higher Ag contents. Sample 5148's Au values are comparable to the Waiotapu sinter deposit in New Zealand (33 ppm). The polymetallic nature of the sinter, linked to the hydrothermal activity and metallogeny of the Văratec deposit, suggests it is associated with low- and intermediate-sulfidation environment (Sillitoe, 2000).

Cisma/Poiana Botizii

The reflected light microscopy revealed the relationships between various metallic minerals, such as hematite being deposited before the sulfides, chalcopyrite being partially replaced by enargite/luzonite, and all these minerals being cut and partially replaced by tennantite.

Regarding the non-metallic minerals defining the hydrothermal alterations, the abundant presence of kaolinite in the enargite-tennantite-chalcopyrite mineral assemblage suggests conditions specific to *intermediate/high sulfidation* environment. Similarly, based solely on the association of metallic minerals enargite with tennantite and galena as in Herja, Kovacs and Tămaș (2020) suggest that the ore from Cisma deposit formed in an *intermediate/high sulfidation* environment.

The chemical analyses of sphalerite from Cisma show similar iron content (2.62-3.21 wt.%) as the values reported by Plotinskaya et al. (2014) for the same deposit (1.3-4.6 wt.%). The analyzed sphalerite has lower Mn content (0.06-0.08 wt.%) and higher Cd content (0.61-0.64 wt.%) compared to first-generation sphalerite separated by Plotinskaya et al. (2014), which had 0.5-0.7 wt.% Mn and 0.2 wt.% Cd. Additionally, Plotinskaya et al. (2014) identified second-generation sphalerite at Cisma by the abundance of chalcopyrite inclusions. This second-generation sphalerite

had higher Mn (0.2 wt.%), similar Fe (1.9-4.5 wt.%), and lower Cd (0.2-0.5 wt.%) compared to the sphalerite analyzed in the present study (Mn: 0.06-0.08 wt.%; Fe: 2.62-3.21 wt.%; Cd: 0.61-0.64 wt.%).

According to Damian and Damian (2003), the ore deposits within the Neogene metallogenic district of Baia Mare contain Zn-rich tetrahedrites and Fe-rich tennantites, with up to 7.69 wt.% Zn and 6.46 wt.% Fe. However, only one of the four tennantite grains currently analyzed contains Zn (0.08 wt.%), near the detection limit (0.065 wt.%), while all analyzed grains have high Fe values (5.70-8.15 wt.%), exceeding the previously mentioned upper limit. The tennantite from Cisma has high Fe content (5.70-8.15 wt.%), low Zn content (below detection limit to 0.8 wt.%), and no Mn. These chemical characteristics can be interpreted as indicators of the *high-sulfidation* nature of the ore (Kovacs and Tamaș, 2020).

The Ag content of tennantite from Cisma (0.35-0.60 wt.%) is consistent with previous data reported by Damian and Damian (2003), who mentioned that ores from the Baia Mare district have silver contents in tetrahedrite-tennantite ores of less than 2 wt.%.

The reflected light optical microscopy observations (Andras, 2017) and the semi-quantitative analyses using electron microprobe scanning (Kovacs and Tămaș, 2018), converge towards the validation of the presence of enargite-type minerals in the Băiuț mining area. The acquired EPMA results, which were presented by Kovacs and Tămaș (2020) represent the first quantitative evidence confirming the presence of enargite/luzonite minerals in the Neogene metallogenic district of Baia Mare.

SEM-BSE images captured by Kovacs and Tămaș (2020) reveal enargite/luzonite grains with various shades of gray, indicating the chemical heterogeneity of the mineral grains, particularly in arsenic (As) and antimony (Sb). Darker areas, such as points 5-7 and 11-14, have lower Sb content (0.27-2.42 wt.%), while lighter areas (points 8-10) exhibit higher Sb content (7.17-8.74 wt.%).

The definite mineralogical identification of whether the grains correspond to enargite or luzonite remains uncertain. Kovacs and Tămaș (2020) cited Uytenbogaardt and Burke (1971) and Pracejus (2015), stating that the differentiation between enargite and luzonite based on microscopic observations is challenging due to their nearly identical optical properties.

Regarding the compositional variation of enargite and tennantite at Cisma, Kovacs and Tămaș (2020) discuss their findings by using the chemical data plotted in the diagram proposed by Ciobanu et al. (2005). According to this approach, Kovacs and Tămaș (2020) suggest the presence

of tennantite and enargite minerals in the Cisma deposit. More precisely, the composition of the analyzed mineral grains suggests intermediate phases closer to the enargite/luzonite end-member, and approaching the compositional pole of tennantite, respectively.

Enargite (Cu_3AsS_4) crystallizes in the orthorhombic system, famatinite (Cu_3SbS_4) in the tetragonal system, while luzonite (Cu_3AsS_4) also crystallizes in the tetragonal system.

Based on electron microscopy analyses, Pósfai and Sundberg (1998) conclude that enargite and luzonite are frequently mixed at the atomic level. Previously, Gaines (1957) and Springer (1969) suggested differentiation between enargite and luzonite based on chemical analyses, specifically noting that if the Sb content is below 6 wt.%, the mineral analyzed corresponds to enargite. According to the results obtained for the ore from the Cisma area and following the criteria proposed by Springer (1969) and Pósfai and Sundberg (1998), the analysis points 8, 9, and 10, with Sb contents (in wt.%) of 8.74, 7.17, and 8.38 exceed the 6 wt.% limit mentioned by Springer (1969). In contrast, the values obtained for the points 1, 2, and 3, expressed in wt.% and coded at 6.15, 6.08, and 5.94, respectively, are very close to tthe 6 wt.% limit. According to Kovacs and Tămaș (2020), these values indicate the presence of enargite and luzonite in the Cisma area, marking the first mention of these minerals in the Baia Mare metallogenic district based on quantitative chemical analyses.

According to the study by Pósfai and Buseck (1998), when enargite coexists with luzonite, luzonite typically contains more Sb than enargite. Pósfai and Buseck (1998) also state that the enargite coexisting with the luzonite-famatinite contains less than 3.3 wt% Sb. Considering these observations, the EPMA points 1-4 with Sb contents ranging from 4.84 wt% to 6.15 wt% represent luzonite, while the EPMA points 5-7 and 11-14, with Sb contents ranging from 0.27 to 2.42 wt.% correspond to enargite (Kovacs and Tămaș, 2020).

Pfitzner and Bernert (2004) investigate the Cu_3AsS_4-Cu_3SbS_4 systems regarding the formation of mixed crystals using X-ray analysis. The crystal structure of the $Cu_3As_xSb_{1-x}S_4$ produced crystals varies distinctly with the value of x. Specifically, in the synthetic system $Cu_3As_xSb_{1-x}S_4$, there are two distinct regions based on the value of $x = 0.8$:

- the compositions with $x < 0.8$ crystallize as famatinite, in the tetragonal system.
- the compositions with $x > 0.8$ crystallize as enargite, in the orthorhombic system (Pfitzner and Bernert, 2004).

The Sb-richest natural enargite described has the composition $Cu_3As_{0.8}Sb_{0.2}S_4$ (Pósfai and Buseck, 1998). This finding is consistent with the experimental results obtained by Pfitzner and Bernert (2004), suggesting that the experimentally identified compositional limit coincides with the findings highlighted by laboratory analyses on natural material. It should be noted that the calculated average chemical formula of enargite from Cisma is $(Cu_{2.97},Fe_{0.06},Zn_{0.004})_{\Sigma=3.03}(As_{0.80}, Sb_{0.14})_{\Sigma=0.94} S_{4.03}$ (Kovacs and Tămaş, 2018), representing the boundary point between the two types of chemical compositions corresponding to distinct crystal structures. Referring to the As and Sb values expressed in wt.% corresponding to the average chemical composition of enargite from Cisma, these are 15.20 wt.% for As and 4.16 wt. % for Sb, which correspond to the value x=0.8 for As identified by Pósfai and Buseck (1998) and Pfitzner and Bernert (2004) as the discriminant between famatinite and enargite crystal structures.

Based on the reasoning above, the conclusions can be drawn as follows (Fig 10.1): i) famatinite is characterized by an As content < 15.20 wt%; ii) enargite coexisting with famatinite has an Sb content less than 3.3 wt%, while luzonite exhibits variable Sb content.

Considering the previous conclusions, it can be stated that: i) EPMA analysis points numbered 1, 2, 3, and 8, 9, 10 correspond to famatinite; ii) EPMA analysis points numbered 5, 6, 7, and 11, 12, 13, 14 correspond to enargite; while iii) EPMA analysis point numbered 4 corresponds to luzonite, as shown in Fig. 10.1.

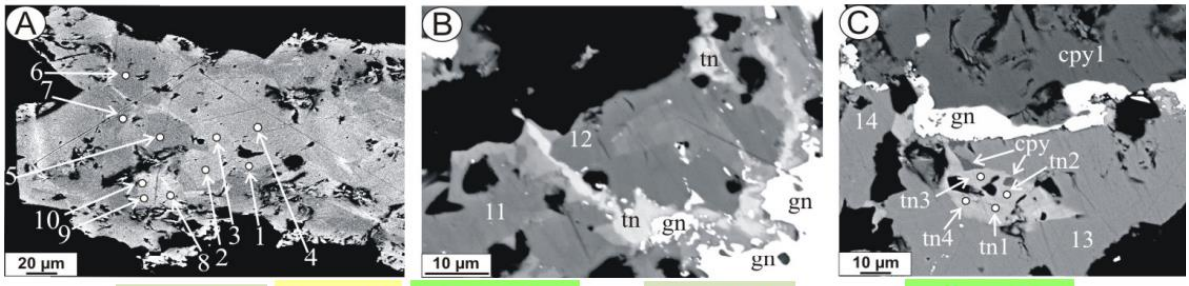

	Famatinit	Luzonit	Enargit				Famatinit			Enargit				
No.	1	2	3	4	5	6	7	8	9	10	11	12	13	14	A
Cu	47.41	47.51	47.89	47.80	48.25	47.90	48.39	47.11	47.50	47.19	47.50	46.93	47.44	47.67	47
Ag	0.00	-	0.00	-	-	-	-	0.00	0.00	-	-	0.30	-	-	
Zn	0.00	0.00	0.00	0.00	0.00	0.00	0.00	0.00	0.00	0.00	0.37	0.67	-	0.00	0.
Fe	0.37	0.26	0.19	0.22	0.54	1.32	0.53	0.25	0.29	0.29	1.43	1.32	2.61	2.29	0.
As	12.92	14.35	14.17	15.30	16.68	16.55	16.91	12.52	13.20	12.07	16.31	16.17	17.96	17.71	15
Sb	6.15	6.08	5.94	4.84	2.10	2.04	1.65	8.74	7.17	8.38	2.42	2.20	0.27	0.27	4.
S	34.57	32.24	32.33	32.51	32.55	32.75	33.18	31.98	32.53	32.68	32.12	32.29	32.85	32.39	32
Total	101.42	100.44	100.5	100.67	100.12	100.56	100.66	100.60	100.69	100.61	100.15	99.88	101.13	100.33	10(

Fig. 10.1. The correspondence between the SEM-BSE images obtained by the electronic microscope by Kovacs and Tămaș (2020), which include the positions of EPMA analysis points and the chemical data extracted from the same publication, but distinctly marked for famatinite, enargite, and luzonite highlighted within the Cisma deposit.

In conclusion, reinterpreting the data published by Kovacs and Tămaș (2020), we have concluded that besides enargite as described by these authors, the ore from Cisma also contains both famatinite and luzonite.

Lead isotopic composition

According to Marcoux et al. (2002), the Neogene epithermal deposits in the Baia Mare metallogenic district generally exhibit homogeneous lead isotopic compositions, similar to those of the calc-alkaline volcanic rocks from the district. This observation forms the basis of Marcoux et al.'s (2002) interpretation, suggesting a magmatic signature for the lead within the ores.

However, the cited author also notes that magmas in the Baia Mare district indicate some crustal contribution due to crustal assimilation.

The ores within the Băiuț metallogenic district are heterogeneous, exhibiting significant variations. Additionally, these ores possess lead isotopic signatures that distinguish them from the rest of the Baia Mare district. The ores from Breiner and one sample from Văratec show lead isotopic ratios closer to those of the Baia Mare metallogenic district, while the remaining ores, specifically Cisma and another one from Văratec, exhibit significantly less radiogenic lead isotopic signatures, with Cisma's being even less radiogenic than the Paleozoic VMS ores from Baia Borșa district.

The distribution of the lead isotopic ratios of the ores within the Băiuț metallogenic field compared to those from the Neogene Baia Mare and Baia Borșa districts, and the Paleozoic ores from Baia Borșa, suggests that the lead in Băiuț ores originates from sources characterized by greater heterogeneity. Specifically, the isotopic ratios of ores from Breiner, Văratec, and Cisma diverge significantly from those of the volcanic rocks, considered by Marcoux et al. (2002) as the main source of Pb of the Neogene epithermal deposits in the Baia Mare district. Moreover, the less radiogenic lead isotopic composition of the ores in Cisma deposit suggests that the lead source has an isotopic composition similar to that of the mantle field defined by Zartman and Doe (1981).

A possible explanation for the lead isotopic composition heterogeneity of the Băiuț ores including the less radiogenic character of Cisma, which contrasts with the more radiogenic ore samples from Breiner and of a sample from Văratec is that the lead source is a crust with high variability, containing less radiogenic Pb isotopic composition, i.e., mantle-like and/or oceanic island volcanic rocks and lithologies with more radiogenic lead isotopic composition (upper crust type according to Zartman and Doe (1981), from which magmas and/or hydrothermal fluids assimilated lead.

11. Conclusions

The Breiner deposit, located in the western part of the Băiuț metallogenic field, is characterized by a wide range of hydrothermal breccias illustrating diverse relationships between hydrothermal cement and clasts. These include hydrothermal breccias with clasts of sedimentary rocks, breccias with clasts of re-brecciated breccias, etc., described for the first time in this deposit. Besides hydrothermal breccias, brecciated and un-brecciated banded vein and vuggy silica textures have also been identified. Microscopic observations revealed clasts of clayey nature, sandstones, and metamorphic fragments.

Regarding the hydrothermal alterations in the Breiner deposit, it was observed that silicification occurs simultaneously with brecciation, while carbonatation postdates the silicification. The ore mineralogy is simple, with pyrite, sphalerite, galena, and chalcopyrite. The presence of these metallic minerals, along with realgar and orpiment (Edelstein et al., 1992; Mariaș, 2005), suggests that the ores at Breiner formed in a transition environment from intermediate to high sulfidation conditions. The geochemical analyses of the samples indicate relatively consistent and significant gold contents, with most samples showing values >1 ppm Au, along with elevated levels of base metals (Cu: up to 7.27%; Pb: up to 4890 ppm; Zn: up to 2080 ppm). The highest concentrations of precious metals were notably found in hydrothermal breccias, with values reaching up to 6.15 ppm Au and 108 ppm Ag.

The Văratec deposit is characterized by a wide spectrum of hydrothermal breccias (e.g., polymictic with clasts of sedimentary rocks, open space breccias, etc.) not previously described in the literature. Additionally, banded ores with red quartz gangue and vuggy silica are present. Microscopic examination reveals hydrothermal alterations including silicification, adularia alteration, sericitization, and carbonatation, occurring in the following succession: silicification, adularia alteration, sericitization, and carbonatation. Based on the metallic minerals identified (pyrite, chalcopyrite, sphalerite, galena, tetrahedrite, quartz, adularia, hematite, quartz gangue), the majority of the Văratec ore fits to the ore deposition stages 1 and 3 defined by Bailly et al. (1998) at the Baia Mare district scale.

The highest Au grade in Văratec, and for the entire Băiuț metallogenic field, was found in a banded ore (59.1 ppm); another 6 samples exceed 8 ppm Au. Besides being auriferous, Văratec is confirmed as argentiferous and polymetallic. Native gold occurrences are notably common in hydrothermal breccias.

Within the Văratec deposit, a large siliceous sinter has been discovered, named Văratec Vest sinter. It measures approximately 600 m in length and 30-50 m in width, significantly larger than those described by Mariaș (2005) in the Cavnic area. This sinter deposit exhibits a variety of textures (massive sinter, banded textures, vuggy silica textures, clast-supported breccias), reflecting the dynamic nature of the hydrothermal system responsible for its formation. The geochemical analyses of sinter samples revealed significant contents of As, Cu, and Sb, while its gold and silver content is very minor. A siliceous sinter sample (float) yielded high Au contents (61.9 ppm).

The samples collected from the Cisma deposit represent various typologies: hydrothermal breccias with clasts of sedimentary rocks and sulfide nests accompanied by quartz sequences; polymetallic ores with brecciated texture; hydrothermal breccias with pyrite cement; open space breccias; polymictic breccias; vein structures; and vuggy silica. Petrographic studies highlighted the presence of pyrite, chalcopyrite, galena, hematite, tennantite, and enargite associated with gray, white, or violet hydrothermal quartz. The sulfides postdate the hematite; the enargite/luzonite replaces the chalcopyrite, and were followed by tennantite.

The mineralogy of the Cisma ore has greatly benefited from the chemical analyses at the electron microprobe (EPMA). These analyses confirmed the presence of the tetrahedrite-tennantite group minerals, i.e., enargite, famatinite, and luzonite. Based on microchemical analyses, these minerals were described for the first time in the Cisma deposit. Except for the identification of enargite by X-ray diffraction at Herja (Kovacs and Tămaș, 2020), the minerals enargite, famatinite, and luzonite are described for the first time at the scale of the Baia Mare metallogenic district based on quantitative chemical analyses.

Kaolinite was identified by X-ray diffraction in a mineralogical association with enargite-tennantite-chalcopyrite. Geochemical analyses conducted on samples from Cisma indicate a consistent presence of gold, with 13 samples showing concentrations above 1 ppm, reaching a maximum of 4.78 ppm.

Lead isotopic analyses conducted on ore samples from the Băiuț metallogenic field indicate the heterogeneity of the lead isotopic ratios, spanning a wide range of values, i.e., 18.23 - 18.88 for $^{206}Pb/^{204}Pb$, 15.26 - 15.7 for $^{207}Pb/^{204}Pb$, and 37.92 - 39.2 for $^{208}Pb/^{204}Pb$. The samples from the Băiuț area exhibit lead isotopic signatures distinct from those of the ores found elsewhere in the Baia Mare metallogenic district.

Specifically, the ore samples from Breiner and one sample from Văratec show isotopic signatures closer to those typical of the Baia Mare district (albeit still distinct). In contrast, the Cisma deposit and another sample from Văratec display less radiogenic lead isotopic signatures. These results, indicating the less radiogenic nature of the ores from Cisma, suggest that the lead source is heterogeneous, derived primarily from crustal sources rather than from the magmas responsible for the volcanism in the Gutâi Mountains, which represent the main lead source for the rest of the ores within the Baia Mare metallogenic district.

References

András, K. (2017). Studiul mineralogic al minereurilor din perimetrul Băiuț (județul Maramureș), cu privire specială asupra zăcămintelor Văratec, Cisma, Coasta Ursului, Johan Hell, Breiner și Poiana Botizei. Dizertație de masterat, University Babeș-Bolyai, Cluj-Napoca.

Bailly, L., Milési, J.P., Leroy, J., Marcoux, E. 1998. Les minéralisations épithermales à Au-Cu-Zn-Sb du district de Baia Mare (Nord Roumanie): nouvelles données minéralogiques et microthermométriques (in French with English summary). Académie des Sciences, Géomatériaux, Paris, 327: 385-390.

Borcoș, M., Gheorghiță, I. 1976. Neogene hydrothermal ore deposits in the volcanic Gutâi Mountains. IV. Băiuţ-Văratec-Botiza metallogenic field. Revue Roumaine de géologie, géophysique et géographie, Série de géologie, 20(2): 197-209.

Borcoș, M., Gheorghiță, I., Mândroiu, V., Volanschi, E. 1977. Considerații privind procesele metalogenetice desfășurate în extremitatea estică a Munților Gutâi (Zăcământul Băiuț-Văratec).. Studii Tehnice şi Economice, Seria A, 11: 53-96.

Ciobanu, C.L., Cook, N.J., Capraru, N., Damian, G., Cristea, P. (2005). Mineral assemblages from the veins salband at Săcărâmb, Golden Quadrilateral, Romania: I. Sulphides and sulphosalts. Geochemistry, Mineralogy and Petrology, 45, 47–55.

Costin, D. 2000. Major Elements Geochemistry of the Breiner Băiuţ Ore Deposits (Gutâi Mts. Eastern Carpathians). Studia Universitatis Babes-Bolyai, Geologia, 45(1): 56-66.

Costin, D. 2003. Compositional data on bournonite–CuPbSb3 from Văratec ore deposit, Băiuţ mine field, Eastern Carpathians, Romania. Studia Universitatis Babes–Bolyai, Geologia, 48(1): 45-54.

Costin, D., Vlad, Ş. 2005. Ore formation at Văratec–Băiuţ, Baia Mare region, East Carpathians, Romania. Geochemistry, Mineralogy and Petrology, 43: 64-68.

Costin, D. 2007. Genetic factors and environmental impact of acid mine drainage at Văratec Băiuţ mine, Baia Mare district, Romania. Studia Universitatis Babeş-Bolyai, Ambientum, 1(1-2): 75-85.

Csontos, L. 1995. Tertiary tectonic evolution of the Intra-Carpathian area: a review. Acta Vulcanologica 7(2): 1–15.

Csontos, L., Nagymarosy, A., Horváth, F., Kováč, M., 1992. Cenozoic evolution of the Intra-Carpathian area: a model. Tectonophysics 208: 221–241.

Csontos, L., Nagymarosy, A. 1998. The Mid-Hungarian Line: a zone of repeated tectonic inversions. Tectonophysics, 297(1-4): 51-71.

Damian, F., Damian, G. 2004. Mineral parageneses of the hydrothermal ore deposits from Baia Mare area Romania. Scientific Bulletin of North University Centre of Baia Mare, Series D, Mining, Mineral processing, Non-ferrous metallurgy, Geology and environmental engineering, 18: 155-172.

Damian, G., Damian, F., Konečný, P., Kollárová, V. 2016. A new occurrence of wolframite-ferberite in Romania. Romanian Journal of Mineral Deposits, 89(1-2): 49-54.

Edelstein, O., Bernád, A., Kovacs, M., Crihan, M., Pécskay, Z. (1992). Preliminary data regarding the K-Ar ages of some eruptive rocks from Baia Mare Neogene volcanic zone. Revue Roumaine de géologie, géophysique et géographie, Série de géologie, 36, 45-60.

Fülöp, A. (2002) Facies analysis of the volcaniclastic sequence built up above the 15.4 Ma rhyolitic ignimbrites from Gutâi Mts., Eastern Carpathians. Studia Universitatis BabeşBolyai, Geologia, Special issue 1, 199–206.

Fülöp, A. (2003) The begining of volcanism in the Gutâi Mts.: Paleovolcanic and paleosedimentological reconstruction. Editura Dacia Cluj-Napoca 134 pp. (in Romanian).

Grancea, L., Bailly, L., Leroy, J., Banks, D., Marcoux, E., Milesi, J.P., Cuney, M., Andre, A.S., Istvan, D., Fabre, C. (2002). Fluid evolution in the Baia Mare epithermal gold/polymetallic district, Inner Carpathians, Romania. Mineralium Deposita, 37, 630-647.

Gurău, A., Roşu, N., Bălaşa, E., Bordea, R. (1970). Considerations regarding the structure and genesis of the Borzaș ore deposit (Baia Mare). Dări de Seamă ale Ședințelor Institutului Geologic, 56 (2 for 1968-1969), 27-48.

Iancu, O.G., Kovacs, M. (2010). Ore deposits and other classic localities in the Eastern Carpathians: From metamorphics to volcanics. Acta Mineralogica–Petrographica, Field Guide Series, 19, 1–55.

Iştvan, D., Vârşescu, I., Halga, S., Grancea, L. (1995). Gold-silver epithermal levels and associations in the eastern area of the Gutâi Mts. and in the Văratec Mts. (Firiza-Botiza area), East Carpathians, Romania. Studia Universitatis Babes-Bolyai, Geologia, 40 (1), 195-210.

Lang, B., Edelstein, O., Steinitz, G., Kovacs, M., Halga, S. (1994). Ar-Ar dating of adularia–A tool in understanding genetic relation between volcanism and mineralization: Baia Mare area (Gutâi Mountains), Northwestern Romania. Economic Geology, 89, 174-180.

Kovacs, M., Edelstein, O., Gabor, M., Bonhomme, M., Pécskay, Z. (1997b). Neogene magmatism and metallogeny in Oaș–Gutâi–Ţibleș Mts.; a new approach based on radiometric datings. Romanian Journal of Mineral Deposits, 78, 35–45.

Kovacs, M., Fülöp, A. (2010). Baia Mare metallogenetic district. In G. Iancu and M. Kovacs (Eds.), Ore deposits and other classic localities in the Eastern Carpathians: From metamorphics to volcanics. Acta Mineralogica-Petrographica, Field Guide Series, 19, 5-13.

Kovacs, M., Fülöp, A., Seghedi, I., & Pécskay, Z. (2021). Architecture of volcanic plumbing systems inferred from thermobarometry: A case study from the Miocene Gutâi Volcanic Zone in the Eastern Carpathians, Romania. Lithos, 396-397, 106191. doi:10.1016/j.lithos.2021.106191.

Kovács, R., Tămaș, C.G. (2018). New geochemical data and mineralogical interpretation for cisma ore deposit, gutâi mountains. Rom. J. Mineral Deposits, vol. 91 (2018), No. 1-2, p. 43-47.

Kovács, R., Tămaș, C.G. (2020). Cu3(As,Sb)S4 minerals from the Baia Mare metallogenic district, Eastern Carpathians, Romania - a case study from the Cisma ore deposit. Geological Quarterly, 64 (2), 263–274. doi: 10.7306/gq.1529.

Manilici, V., Giușcă, D., Stiopol, V. (1965). Studiul zăcământului de la Baia Sprie (regiunea Baia Mare). Memorii, vol. VII, p. 1-95.

Marcoux, E., Grancea, L., Lupulescu, M., Milesi, J.-P. (2002). Lead isotope signatures of epithermal and porphyry-type ore deposits from Romanian Carpathians Mountains. Mineralium Deposita, 37, 173-184.

Mariaș, F. (2005). Metalogenia districtului minier Baia Mare, model bazat pe sistemul hidrotermal Cavnic (Maramureș), evaluări comparative cu alte sisteme epitermale din lume. Editura Cornelius, 450 p.

Márton, E., Pogác, P., & Tunyi, I. (1992). Paleomagnetic investigations on Late Cretaceous-Cenozoic sediments from the NW part of the Pannonian Basin. Geologica Carpathica, 43, 363–369.

Mârza, I. (2002). Geneza zăcămintelor de origine magmatică. 4. Metalogenie hidrotermală. Presa Universitară Clujeană, 516 p.

Neubauer, F., Höck, V., & Miller, C. (2005). Structure and kinematic evolution of the Giurgeu Batholith (Eastern Carpathians, Romania): implications for the kinematic evolution of the Carpathian–Pannonian system. Tectonophysics, 410(1-4), 407-428.

Panaiotu, C., Pécskay, Z., Panaiotu, C., 1996. Which is the time of rotation? Review of paleomagnetic and K-Ar data from Romania. Mitteilungen Gesellschaft der Geologie und Bergbaustudenten 41: 125.

Pătraşcu, S., Panaiotu, C., Şeclăman, M., Panaiotu, C.E. (1994). Timing of rotational motion of Apuseni Mountains (Romania): Paleomagnetic data from Tertiary magmatic rocks. Tectonophysics, 233, 163–176.

Pfitzner, Arno, Thomas Bernert. (2004). The system Cu3AsS4–Cu3SbS4 and investigations on normal tetrahedral structures. Zeitschrift für Kristallographie - Crystalline Materials, 219, 20-26.

Plotinskaya, O.Y., Prokofiev, V.Y., Damian, G., Damian, F., Lehmann, B. (2012). The Cisma deposit, Băiuţ district, Eastern Carpathians, Romania: sphalerite composition and formation conditions. Carpathian Journal of Earth and Environmental Sciences, 7(2), 265–273.

Pop, N., Pop, V., Kovács-Pálffy, P. (1982). Date mineralogice, petrografice şi geochimice asupra tufurilor vulcanice zeolitizate din bazinele Şimleu, Oaş şi Izei. Revista Mine, Petrol şi Gaze, 33(4), 175-182, Bucureşti, România.

Pósfai, M., Sundberg, M. (1998). Stacking disorder and polytypism in enargite and luzonite. American Mineralogist, 83, 365–372.

Pósfai, M., Buseck, P. (1998). Relationships between microstructure and composition in enargite and luzonite. American Mineralogist, 83, 373–382.

Pracejus, B. (2015). The Ore Minerals under the Microscope: An Optical Guide. 2nd edition, Elsevier.

Rodgers, K.A., Browne, P.R.L., Buddle, T.F., Cook, K.L., Greatrex, R.A., Hampton, W.A., Herdianita, N.R., Holland, G.R., Lynne, B.Y., Martin, R., Newton, Z., Pastars, D., Sannazarro, K.L., Teece, C.I.A., 2004. Silica phases in sinters and residues from geothermal fields of New Zealand. Earth Sci Rev 66:1–61.

Royden, L.H. (1988). Late Cenozoic tectonics of the Pannonian Basin system. In L. Royden & F. Horváth (Eds.), The Pannonian Basin. A study in basin evolution. AAPG Memoir, 45, 27–48.

Săndulescu, M., Russo-Săndulescu, D., 1981. Geological map of Romania, 1:50 000, sheet 19c. Institutul de Geologie și Geofizică, București.

Seghedi, I., Balintoni, I., Szakács, A., 1998. Interplay of tectonics and Neogene post-collisional magmatism in the Intracarpathian area. Lithos 465: 483–499.

Springer, G. (1969). Compositional variations in enargite and luzonite. Mineralium Deposita, 4, 72–74.

Tămaș, C.G., 2002. Structuri de „breccia pipe” asociate unor zăcăminte hidrotermale din România. Teză de doctorat, Universitatea Babeș-Bolyai, Cluj-Napoca, România, 336 p.

Tischler, M., Gröger, H.R., Fügenschuh, B., Schmid, S.M., 2007. Miocene tectonics of the Maramureş area (Northern Romania): implications for the Mid-Hungarian fault zone. International Journal of Earth Sciences, Geologische Rundschau, 96: 473-496.

Uytenbogaardt, W., Burke, E.A.J. (1971). Tables for microscopic identification of ore minerals. 2nd ed. Elsevier, Amsterdam.

Zartman, R.E., Doe, B.R. (1981). Plumbotectonics – the model. Tectonophysics, 75, 135-162.